A re-examination of the mechanism of thermosonic copper ball bonding on aluminium metallization pads

H. Xu[a], C. Liu[a], V.V. Silberschmidt[a], S.S. Pramana[b], T.J. White[b], Z. Chen[b]

[a]Wolfson School of Mechanical and Manufacturing Engineering, Loughborough University, Loughborough, LE11 3TU, UK

[b]School of Materials Science and Engineering, Nanyang Technological University, Nanyang Avenue, Singapore 639798, Singapore

Abstract

The nano-scale interfacial characteristics of thermosonic copper ball bonding on aluminium metallization were investigated. It was found that ultrasonic vibration swept oxides of aluminium and copper from parts of the contact area, promoting the formation of intermetallic compound Al_2Cu (approx. 20 nm thick). Where oxides persisted, an amorphous aluminium oxide layer connected with a crystalline copper oxide. It is estimated that ultrasonic vibration caused an effective local temperature increase to 465°C that accelerated interdiffusion and enhanced the formation of Cu-Al intermetallics.

Keywords: Thermosonic bonding mechanism; Interfacial structure; Intermetallic compounds.

Thermosonic copper ball bonding to aluminium provides excellent electrical and mechanical properties for high-speed, high-power devices and fine-pitch microelectronic applications, and may prove a cost-effective alternative to gold bonding [1]. The relationship between process parameters and bondability [2-5] and the reliability of bonds subjected to thermal cycling and aging [6-11] are well studied. However, the fundamental principles of bonding remain poorly understood [12]. They are commonly described as fretting [13] or micro-slip [14, 15] processes, where the former considers bonding to be promoted by interfacial sliding that cleans and heats metallization pad, while the latter predicts preferential slips and bonding at the interfacial periphery. However, neither mechanism is supported by examination of copper-aluminium boundaries at near-atomic scales.

Intermetallic formation at the Cu-Al bond should improve strength, and five alloys ($Al_2Cu(\theta)$, $AlCu(\eta_2)$, $Al_3Cu_4(\zeta_2)$, $Al_2Cu_3(\delta)$ and $Al_4Cu_9(\gamma_2)$) are possible [9], but excessive growth will degrade mechanical integrity [1, 10, 16]. For example, Kim, *et al.* [10] found that after aging for 100 hours at 250°C the IMC was approx. 1.2 μm. The corresponding shear strength was about 80% of that in the as-bonded state, and the failure site was the interface between Cu-Al IMC and SiO_2/Si. Although scanning electron microscopy (SEM) found no Cu-Al intermetallics after bonding [6, 7], extremely thin alloy domains are difficult to detect with this method. Therefore, this study was undertaken to examine the interfacial characteristics of the Cu-Al boundary in fine detail.

In these experiments, a copper wire (99.99 wt.% / 25.4 μm diameter) was bonded to an aluminium metallization pad (1 μm thick) on a silicon chip using an ASM Eagle 60 ball/wedge automatic bonder at an ultrasonic frequency of 138 kHz. An electronic flame-off (EFO) process produced a spherical ball under a protective gas mixture (95% N_2 + 5% H_2) introduced at the rate of 0.8 L/min, to limit the oxidation of copper. Bonding was complete within 0.025 s using a combination of transverse ultrasonic vibration (150 mW), an external force normal to the interface (60 gram), and heat (200^{o}C). Shear (180.7 MPa) and pull (68.5

MPa) tests confirmed the high strength of Cu-Al bonds. To study the interfaces in detail, region-specific transmission electron microscope (TEM) sections of the Cu-Al interfaces were prepared using a dual-beam focused ion beam (FIB).

Cu-Al interfaces contain two types of morphologies – labelled as A and B in Figure 1 – a with fractions of approx. 70% and approx. 30%, respectively. Both morphologies are gap-free and void-free. Here, voids signifies Kirkendall voids which were reported to be present at nanoscale at the Au/Al interface of thermosonic Au-Al bonds [17], while a gap means that two metals are not metallurgically bonded and there is a narrow and relatively long area between their free surfaces. The latter was found at sub-micro scale in the central contact area of thermosonic Cu-Al bonds in our previous study when the bonding parameters were not optimized. In region A three layers can be distinguished with those closest to aluminium being amorphous (A-1 and A-2), while layer A-3 abutting copper is crystalline (Figure 2a). Scanning (S)TEM - energy dispersive X-ray spectrometry (EDX) suggests A-1 is aluminium oxide and A-2 was an aluminium-rich phase (Table 1). Since a compact oxide film with thickness 5 nm - 20 nm forms on aluminium in air [18], the layer of amorphous alumina with thickness of 10-15 nm (A-1, Figure 2a) is believed to exist before bonding and not be removed during bonding.

In detail, region A-A in Figure 2a consists of two distinct electron interference patterns (Figure 2b) with fast Fourier transform (FFT) analysis of these regions consistent with copper metal (a = 0.361 nm) and CuO ($C12/c1$, a = 0.465 nm, b = 0.341 nm, c = 0.511 nm, β = 99.59°) in agreement with STEM-EDX (Table 1). The copper oxide (~3 nm thick) is thought to form during electronic sparking and ball formation. The amorphous aluminium oxide and copper oxide layers appear contiguous at the atomic scale.

In the second type of Cu-Al interface (region B, Figure 1) the amorphous aluminium oxide was replaced with a layer (approx. 20 nm thick) (Figure 3a), which is crystalline (Figure 3b, c). FFT analysis of the interference lattices are consistent with Al_2Cu (*I4/mcm*, a = 0.496 nm,

b = 0.859 nm and c = 0.848 nm) aligned along [210] orientation forming a boundary with Al (*Fm*-3*m*, a = 0.406 nm) and Cu (*Fm*-3*m*, a = 0.361 nm) in [101] (Figs. 3b, c). The interfaces may be semi-coherent as Al d_{020} = 0.203 nm, $d_{11\text{-}1}$ = 0.234 nm; Al_2Cu d_{002} = 0.244 nm, and d_{121} = 0.237 nm, but a selection of images collected over a range of tilt angles would be required for confirmation.

Since continuous and compact layers of aluminium oxide and copper oxide were present before bonding [12, 19], it is now clear that ultrasonic vibration removes these from some parts of the contact area (such as region B, Figure 1), while in others (such as region A, Figure 1) the oxides were persistent. The contacting surfaces are relatively rough [20], and wear preferentially at the asperities, while oxides remain in surface depressions. Where the oxides are absent, a Cu-Al intermetallic layer forms with Al_2Cu nucleating first. Murali *et al.* [6] and Ratchev *et al.* [7] did not detect Cu-Al intermetallics by SEM due to their extremely small size, however, they can be identified by TEM.

It has been reported that intermetallic growth in Cu-Al bonds follows a parabolic law during thermal aging [8, 10, 16], such that

$$x = (Dt)^{1/2} \tag{1}$$

and

$$D = D_0 \exp(-Q/RT), \tag{2}$$

where x is the IMC thickness at time t, D is the growth rate constant, D_0 is a pre-factor, Q is the activation energy, R is the molar gas constant, and T is the absolute temperature.

According to Xu *et al* [8], Q = 1.01 eV and D_0 = 1.21×10^{-7} m^2/s, for the growth of Cu-Al intermetallics. Consequently, in the present studies with x = 20 nm and t = 0.025 s, the effective (or equivalent) temperature is estimated to be 465°C. The effective temperature includes the temperature T increase caused by mechanical vibration and a decrease in Q as a result of ultrasonic action, but the contribution of each term requires investigation. A previous

in-situ measurement of interfacial temperature using K-type thin film thermocouples yielded 320°C [21]. The higher temperature estimated in this study is for a specific small local region, while the thermocouple measurement is an average over the sensor (20 μm in width). Despite the uncertainty of temperature determination at the interface, it is clear that ultrasonic vibration not only cleaned the contact surface, but also increased the effective local temperature, which improved atomic interdiffusion between Cu and Al.

To summarize, a thermosonic copper ball bonding mechanism that exploits ultrasonic vibration has been found to locally remove aluminium and copper oxides (such as region B, Figure 1), which promotes the Cu/Al adhesion under the bonding pressure. Atomic interdiffusion proceeds in areas where the fresh metals are exposed and in contact. The flash temperature at these regions effectively increases to 465°C due to the atomic motion induced by ultrasonic vibration. This promotes the formation of Cu-Al intermetallic (Al_2Cu) layer and significantly improves the bonding strength. In the regions where oxide remains and no intermetallics exist (such as region A, Figure 1), the aluminium and copper oxides directly connect without voids or gaps.

Acknowledgments

This paper is an output of the PMI2 Project funded by the UK Department for Innovation, Universities and Skills (DIUS) for the benefit of the Singapore Higher Education Sector and the UK Higher Education Sector. The authors also acknowledge Dr Geoff West, Mr Shaode Zhu and Mr Honghui Wang for their advice and assistance with the experiments.

References

[1] S.L. Khoury, D.J. Burkhard, D.P. Galloway, and T.A. Scharr, IEEE Trans. Comp., Hybrids, Manuf. Tech. 13 (1990) 673.

[2] J. Qi, N.C. Hung, M. Li, D. Liu, Scripta Mater. 54 (2006) 293.

[3] Y. Ding, J.K. Kim, P. Tong, Mech. Mater. 38 (2006) 11.

[4] L.T. Nguyen, D. McDonald, A.R. Danker, and P. Ng, IEEE Trans. Comp., Pack. Manuf. Tech. 18 (1995) 423.

[5] A. Shah, M. Mayer, Y. Zhou, S.J. Hong, and J.T. Moon, Microelectron. Eng. 85 (2008) 1851.

[6] S. Murali, N. Srikanth, and C.J. Vath, Mater. Res. Bull. 38 (2003) 637.

[7] P. Ratchev, S. Stoukatch, and B. Swinnen, Microelectron. Reliab. 46 (2006) 1315.

[8] H. Xu, C. Wang, and C. Hang, Acta Metall. Sin. 43 (2007) 125.

[9] C. Xu, T. Sritharan, S.G. Mhaisalkar, Scripta Mater. 56 (2007) 549

[10] H.J. Kim, J.Y. Lee, K.W. Paik, K.W. Koh, W.J, S. Choe, J. Lee, J.T. Moon, Y.J.Park, IEEE Trans. Comp. Pack. Tech. 26 (2003) 367.

[11] S. Murali, N. Srikanth, and C.J. Vath, Mater. Lett. 58 (2004) 3096.

[12] G.G. Harman, Wire Bonding in Microelectronics, Materials, Processes, Reliability, and Yield. Second Ed., McGraw-Hill, New York, 1997.

[13] A.P. Hulst, Weld. J. 57 (1978) 19.

[14] R.D. Mindlin, J. Appl. Mech-T ASME. 18 (1951) 331.

[15] G.G. Harman and J. Albers, IEEE Trans. Parts, Hybrids, Pack. 13 (1977) 406.

[16] W.B. Lee, K.S. Bang, S.B. Jung, J Alloy Comp. 390 (2005) 212.

[17] A. Karpel, G. Gur, Z. Atzmon, W.D. Kaplan, J Mater. Sci. 42 (2007) 2334.

[18] G.E. Totten, D.S. Markenzie, Handbook of Aluminum Volume 1: Physical Metallurgy and Processes, Routledge, New York, 2003.

[19] S.K. Prasad, Advanced Wirebond Interconnection Technology, Springer, New York, 2004.

[20] G. Pugliese, S.M.O. Tavares, E. Ciulli, and L.A. Ferreira, Wear. 264 (2008) 1116.

[21] J. Ho, C. Chen, and C. Wang, Sensor Actuat A-Phys. 111 (2004) 118.

Table Captions

Table 1 STEM-EDX results for regions 1 - 7 in Figure 2a

Regions	O K at.%	Al K at.%	Cu K at.%
1	4.8±10	93.1±2	2.1±2
2	11.2±10	87.4±2	1.4±2
3	55.2±10	43.0±2	1.8±2
4	42.5±10	50.1±2	7.4±2
5	46.6±10	48.0±2	5.4±2
6	44.8±10	11.7±2	43.5±2
7	6.3±10	3.3±2	90.4±2

Table 1

Figure Captions

Figure 1. TEM image of interfacial morphologies of Cu-Al bond.

Figure 2. (a) Details of region A in Figure 1 with three layers between copper and aluminium. (b) Details of region A-A in Figure 2a: region A-A-1 - Cu and region A-A-2 - CuO.

Figure 3. (a) Details of region B in Figure 1 show that the amorphous aluminium oxide layer disappears, and an ~ 20 nm-thick layer of crystalline Al_2Cu introduced. (b) Details of region B-A in Figure 3a. (c) Details of region B-B in Figure 3a.

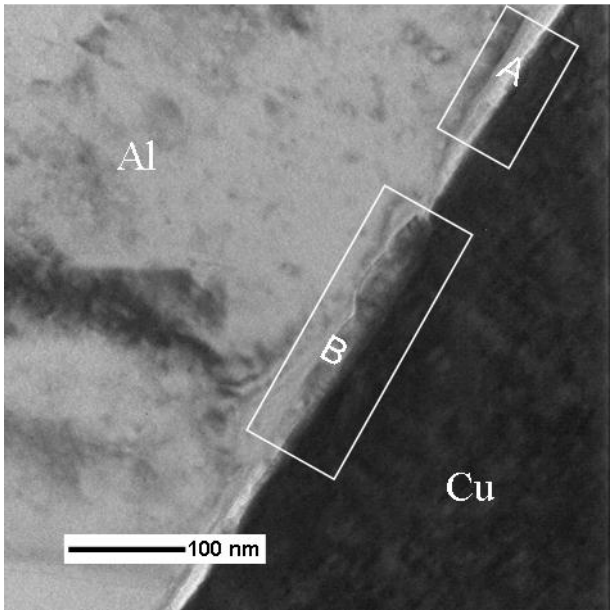

Fig. 1

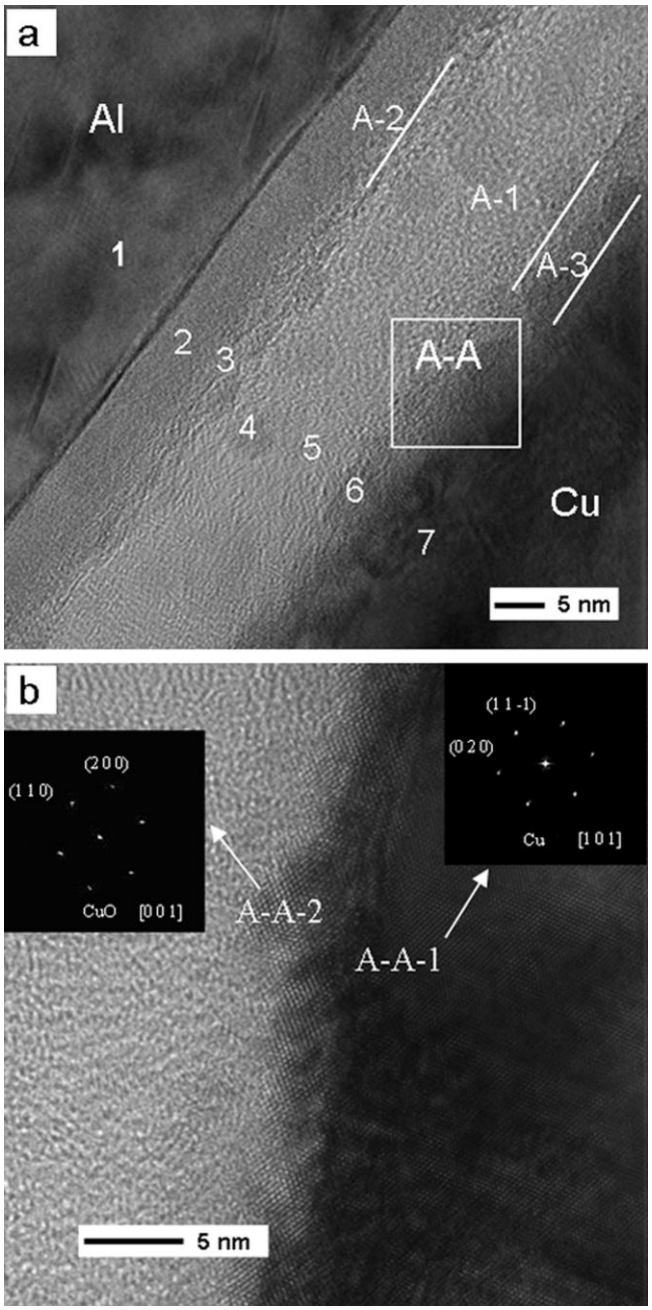
a
Al
A-2
A-1
A-3
1
2
3
A-A
4
5
6
Cu
7
5 nm
b
(200)
(110)
CuO [001]
(11-1)
(020)
Cu [101]
A-A-2
A-A-1
5 nm

Fig. 2

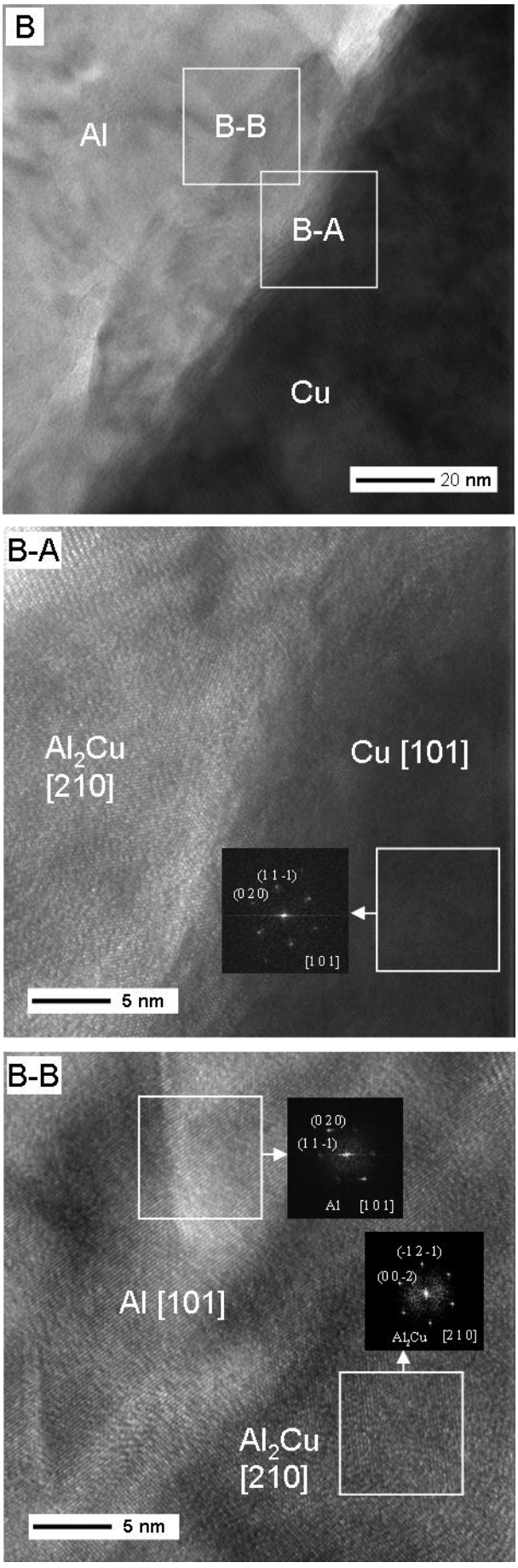
B
Al
B-B
B-A
Cu
20 nm
B-A
Al2Cu
[210]
Cu [101]
(1 1 -1)
(0 2 0)
[1 0 1]
5 nm
B-B
(0 2 0)
(1 1 -1)
Al [1 0 1]
(-1 2 -1)
(0 0 -2)
Al2Cu [2 1 0]
Al [101]
Al2Cu
[210]
5 nm

Fig. 3